



Field evidence for disequilibrium dynamics in preserved fluvial cross-strata: A record of discharge variability or morphodynamic hierarchy?



Sinéad J. Lyster^{a,*}, Alexander C. Whittaker^a, Elizabeth A. Hajek^b, Vamsi Ganti^{c,d}

^a Department of Earth Science and Engineering, Imperial College London, London, UK

^b Department of Geosciences, The Pennsylvania State University, PA, USA

^c Department of Geography, University of California Santa Barbara, CA, USA

^d Department of Earth Science, University of California Santa Barbara, CA, USA

ARTICLE INFO

Article history:

Received 13 May 2021

Received in revised form 7 December 2021

Accepted 20 December 2021

Available online 4 January 2022

Editor: J.-P. Avouac

Keywords:

fluvial systems
bedforms
cross strata
hydrodynamics
morphodynamics
discharge variability

ABSTRACT

Bedforms preserved in the rock record can provide detailed information on the morphologies and hydrodynamics of ancient fluvial systems on Earth and other planets. Existing process-product relations for bedform preservation assume that fluvial cross strata reflect conditions under which bedforms were equilibrated with the prevailing flow, i.e., steady-state conditions. However, recent theoretical and experimental observations indicate that enhanced bedform preservation can occur in non-steady state, or disequilibrium, conditions, and it is currently unclear how prevalent disequilibrium dynamics are in preserved fluvial strata at outcrop scale. Here we explore whether steady-state assumptions are appropriate for ancient fluvial systems by evaluating the nature of bedform preservation in well studied fluvial deposits of three Upper Cretaceous (Turonian and Campanian) geologic formations in central Utah, USA: the Blackhawk Formation, Castlegate Sandstone, and Ferron Sandstone. In the field, we made systematic measurements of dune-scale cross-strata to quantify the extent to which preserved cross-sets reflect dune preservation in steady-state conditions. Across the three formations, consistently low coefficients of variation in preserved cross-set thicknesses of 0.25–0.5 are inconsistent with bedform preservation in steady-state conditions, and instead point to fluvial systems in which enhanced bedform preservation occurred in disequilibrium conditions.

Enhanced bedform preservation in dune-scale cross-stratification can be explained by two independent hypotheses: the effect of flashy flood hydrographs on bedform preservation (flood hypothesis) or bedform preservation in the presence of larger migrating barforms (hierarchy hypothesis). We estimated bedform turnover timescales to quantitatively assess these competing hypotheses and contextualize their implications. Under the flood hypothesis, field measurements are consistent with enhanced bedform preservation driven by flashy flood hydrographs with flood durations ranging on the order of hours to a few days, which are consistent with perennial fluvial systems subject to heavy rains and tropical storms. Alternatively, under the hierarchy hypothesis, field measurements are consistent with bedform climb angles that range from 10^{-2} to 10^{-1} , reflecting rapid bar migration. Our work provides a novel way of investigating fluvial discharge variability in the geologic past, and we outline the potential next steps to disentangle the relative controls of flow variability and morphodynamic hierarchy in controlling bedform preservation in ancient fluvial systems.

© 2021 Elsevier B.V. All rights reserved.

1. Introduction

Quantitative reconstructions of palaeohydraulics from fluvial stratigraphy complement qualitative observations of sedimentary

facies to build more complete pictures of palaeo-landscapes on Earth and other planets. In fluvial strata, preserved bedforms, which include ripples, dunes, and unit bars, are crucial to these reconstructions. Bedforms are readily formed on riverbeds across a range of grain sizes (e.g., Carling, 1999; Best, 2005) and their evolution generates cross-stratification – the resultant cross-strata are a fundamental building block of alluvium on planetary surfaces (e.g., Allen, 1982; Edgar et al., 2018). Cross-strata provide

* Corresponding author.

E-mail address: s.lyster17@imperial.ac.uk (S.J. Lyster).

a window to formative conditions in ancient fluvial systems and are routinely used to reconstruct morphologies and hydrodynamics (Holbrook and Wanas, 2014; Ganti et al., 2019; Wang et al., 2020; Lyster et al., 2021); for instance, measurements of dune-scale cross-set thicknesses provide a mechanism to estimate the sizes of dunes active on ancient riverbeds and, therefore, palaeoflow depths (Leclair and Bridge, 2001; Bradley and Venditti, 2017). Moreover, bedform kinematics respond to spatial and temporal changes in flow and sediment transport conditions (e.g., Ten Brinke et al., 1999; Martin and Jerolmack, 2013; Wu et al., 2020), and recent research has highlighted that these changes may be recorded in preserved cross-set geometries (Leary and Ganti, 2020). If we can use geometries of cross-stratification to extract information about water and sediment discharge variability, this would significantly improve our understanding of ancient fluvial systems, including river response to climatic perturbation (e.g., Foreman et al., 2012; Colombera et al., 2017). However, a crucial outstanding challenge in this field of research involves adapting engineering-scale insights, which are typically founded in precisely defined boundary conditions (and which underpin palaeohydraulic reconstructions), to geological scales over which more variability in environmental conditions is typically assumed due to issues of time-averaging and temporal incompleteness in the rock record (e.g., Romans et al., 2016; Straub et al., 2020).

Process-product relationships between bedform evolution and cross-stratal geometries have primarily been studied using small-scale physical experiments and numerical models (Paola and Borgman, 1991; Bridge, 1997; Leclair, 2002; Jerolmack and Mohrig, 2005; Ganti et al., 2013; Wu et al., 2020). Existing models that relate cross-set thicknesses to original bedform heights rely on the assumption that the formative train of bedforms evolved in steady-state conditions under no-net aggradation or with a small bedform climb angle ($<10^{-2}$; gradient in terms of y/x) (Paola and Borgman, 1991; Jerolmack and Mohrig, 2005). For a range of these formative conditions, theory, numerical models, and experimental observations suggest the bedform preservation ratio – defined as the ratio of the average preserved cross-set thicknesses and the average original bedform heights – is a near-constant value of 0.3 (Paola and Borgman, 1991; Leclair and Bridge, 2001; Leclair, 2002; Jerolmack and Mohrig, 2005). Further, these models predict that the coefficient of variation, CV , of cross-set thicknesses has a constant value of 0.88 (Paola and Borgman, 1991; Leclair and Bridge, 2001; Leclair, 2002; Jerolmack and Mohrig, 2005), with Bridge (1997) suggesting that the steady-state model for bedform preservation can be applied so long as the CV of cross-set thicknesses is bounded by 0.88 ± 0.30 . While these insights have primarily been supported by numerical and experimental studies under steady-state conditions (e.g., Leclair, 2002; Ganti et al., 2013; Leary and Ganti, 2020), they are widely applied in field-scale palaeohydrological studies (e.g., Holbrook and Wanas, 2014; Ganti et al., 2019; Wang et al., 2020; Lyster et al., 2021).

However, steady-state conditions, strictly defined, are not commonly observed in natural systems when discharge is variable (e.g., Fielding et al., 2018; Ghinassi et al., 2018; Herbert et al., 2020), or under relatively constant flow conditions in which spontaneously developed features, such as bars, establish complex and locally variable flow conditions that change as bars shift and channels migrate (Reesink et al., 2015; Chamberlin and Hajek, 2019; Ganti et al., 2020; Wysocki and Hajek, 2021). These non-steady, or disequilibrium, conditions are increasingly recognized to be fundamental controls on fluvial behaviour and stratigraphic architecture (Plink-Björklund, 2015; Reesink et al., 2015; Fielding et al., 2018; Ghinassi et al., 2018; Ganti et al., 2020; Herbert et al., 2020; Leary and Ganti, 2020; Wysocki and Hajek, 2021). At the bedform scale, recent theoretical and experimental observations indicate that fluvial cross-strata may preferentially record bedform dynamics in dise-

quilibrium conditions (Reesink et al., 2015; Ganti et al., 2020; Leary and Ganti, 2020), i.e., when flow and bedform evolution are out of phase (cf. Myrow et al., 2018). Bedform disequilibrium conditions are characterized by localized increase in sedimentation rates relative to bedform migration rates, which enhances the preservation of bedforms (Reesink et al., 2015; Ganti et al., 2020; Leary and Ganti, 2020). Cross-sets preserved in disequilibrium conditions have diagnostic geometries that deviate from cross-sets preserved in steady-state conditions: a) restricted range of cross-set thickness distributions such that $CV < 0.88$ and b) elevated bedform preservation ratios (>0.3) such that a larger fraction of the formative topography is preserved in the stratigraphy (Jerolmack and Mohrig, 2005; Leary and Ganti, 2020; Wu et al., 2020).

Two distinct disequilibrium conditions lead to enhanced bedform preservation. First, Leary and Ganti (2020) used experimental data to show that characteristic patterns of dune preservation are found under different conditions of formative flow variability (i.e., the near-instantaneous short-term discharge variability associated with the magnitudes and timescales of individual floods). They demonstrated that dune preservation preferentially occurs during flood recession, and that preserved cross-sets only have geometries that are consistent with steady-state conditions when the formative flow duration (T_f), i.e., the flood recession, is greater than the bedform turnover timescale (T_t) – defined as the time it takes to displace the volume of sediment in a bedform (Myrow et al., 2018). Conversely, when the flood recession is shorter than the bedform turnover timescale, the larger peak flood-equilibrated dunes get abandoned and are minimally reworked during the flood recession and subsequent low flow conditions, which results in a high bedform preservation ratio and low CV for preserved cross-sets (Leary and Ganti, 2020). These conditions are typical in rivers with flashy flood hydrographs (relative to bedform turnover timescales), which are characterised by rapid flow deceleration and, therefore, short flood recessions. We term this the *flood hypothesis* for enhanced bedform preservation. Moreover, Leary and Ganti (2020) showed that it is possible to estimate formative flow durations from preserved cross-sets – this may enable quantitative reconstructions of flood variability from the rock record and augment traditional qualitative methods that rely on facies and architectural models (e.g., Plink-Björklund, 2015). Alternatively, the self-organization of fluvial systems into a morphodynamic hierarchy (e.g., dunes, bars, channels, channel belts) can also result in enhanced preservation of the topography associated with each hierarchical level (Ganti et al., 2020). In this scenario, high bedform preservation ratio and low CV can occur due to localized increase in the angle of climb of bedforms associated with, for example, concurrent migration of dunes and bars (Jerolmack and Mohrig, 2005; Ganti et al., 2013; Reesink et al., 2015; Ganti et al., 2020), which include both unit bars and longer-lived compound bar features. We term this the *hierarchy hypothesis* for enhanced bedform preservation. In both of these scenarios, cross-strata are expected to encode more detailed information about morphodynamic conditions in ancient fluvial systems, which are not accounted for in models that assume bedform preservation occurred in steady-state conditions.

Despite advances in understanding bedform dynamics, the prevalence of bedform disequilibrium dynamics in preserved fluvial strata is currently unclear, partly because we lack detailed field measurements of cross-set geometries and their statistical nature. While a handful of field studies have documented low CV (0.3–0.7) in fluvial cross-strata (Jerolmack and Mohrig, 2005; Colombera et al., 2017; Cardenas et al., 2020; Wang et al., 2020), consistent with bedform disequilibrium dynamics, these data are usually limited to a few outcrop observations for individual geologic formations. Here, we systematically characterize the geometries and statistical nature of dune-scale cross-strata for three Late

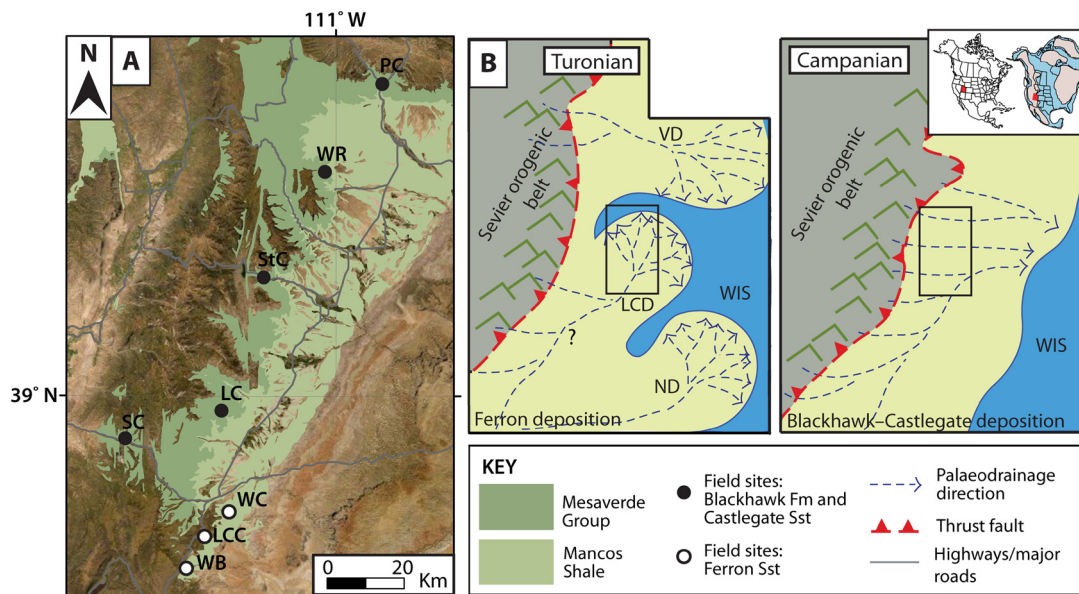


Fig. 1. Study area. A) Field areas in central Utah, U.S.A., which include Last Chance Creek (LCC), Link Canyon (LC), Price Canyon (PC), Salina Canyon (SC), Straight Canyon (StC), Watis Road (WR), Willow Basin (WB) and Willow Creek (WC). LC, PC, SC, StC and WR are field sites from which we obtained data for the Blackhawk Formation and Castlegate Sandstone (Mesaverde Group; black-filled circles). LCC, WB and WC are field sites from which we obtained data for the Ferron Sandstone (Mancos Shale; white-filled circles). B) A conceptual diagram of Utah palaeogeography and palaeodrainage in both the Turonian (left) and Campanian (right). Likely palaeodrainage configurations (and delta progradation) are indicated by dashed blue lines with arrows. The black outlined box in the centre of each palaeogeography indicates the study area (i.e., the approximate position and extent of A). The location of Utah relative to the modern North American continent (left) and the Late Cretaceous North American continent (right) is shown in the inset figure – Utah is highlighted as a red box. LCD = Last Chance delta; ND = Notom delta; VD = Vernal delta; WIS = Western Interior Seaway. Figure adapted from Lyster et al. (2021). (For interpretation of the colours in the figure(s), the reader is referred to the web version of this article.)

Cretaceous geologic formations in central Utah, USA (Figs. 1, 2), to assess the nature of dune preservation. Across all three formations, we show that dune-scale cross-strata are dominated by the preservation of bedform disequilibrium dynamics, which calls into question the use of steady-state assumptions in palaeohydraulic reconstructions. Using these field observations, we reconstruct bedform kinematics (i.e., turnover timescales) and quantify the formative conditions that are consistent with field data under both the flood and hierarchy hypotheses (i.e., flood durations, migration rates). Finally, we evaluate whether it is possible to deconvolve the relative roles of flow variability and morphodynamic hierarchy on enhanced bedform preservation, which may provide a potentially powerful pathway to reconstruct flood variability in ancient fluvial systems, and to evaluate the nature of interactions between dunes, bars, channel migration and channel avulsion in palaeo-channel networks.

2. Study area

In the Late Cretaceous North American continent, rivers draining the Sevier orogenic fold-and-thrust belt delivered sediment to the Western Interior Seaway (WIS) (e.g., Kauffman and Caldwell, 1993) (Fig. 1). We focus on well-studied fluvial strata of the Upper Cretaceous Blackhawk Formation, Castlegate Sandstone and Ferron Sandstone in central Utah, USA (Figs. 1, 2) (cf. Lyster et al., 2021). These strata have distinct architectures and are interpreted to preserve differing fluvial styles; the Ferron Sandstone preserves major meandering trunk channels (Cotter, 1971; Chidsey et al., 2004), while, at the Blackhawk–Castlegate transition, the deposits of single- and multi-thread channels of the Blackhawk Formation (Adams and Bhattacharya, 2005; Hampson et al., 2013; Flood and Hampson, 2014) are capped by the deposits of predominantly braided channels of the Castlegate Sandstone (e.g., Miall, 1993, 1994) (Fig. 1, 2). Moreover, these systems are potentially linked with a monsoonal climate (Fricke et al., 2010; Sewall and Fricke, 2013).

2.1. Blackhawk formation and Castlegate Sandstone, Mesaverde group

The Campanian Blackhawk Formation and Castlegate Sandstone (Figs. 1, 2) represent a series of transverse fluvial systems draining the Sevier orogenic front to the WIS (Pettit et al., 2019), with an additional longitudinal component of drainage from the south-southwest (e.g., Szwarc et al., 2015; Pettit et al., 2019) (Fig. 1b). The lower–middle Campanian Blackhawk Formation is a ledge-forming succession characterized by large fluvial channelized sandstone bodies and abundant floodplain sediments (e.g., Adams and Bhattacharya, 2005; Hampson et al., 2013; Flood and Hampson, 2014) (Fig. 2a–c). These sandstone bodies represent both single- and multi-thread systems, as interpreted from bar architectures (Adams and Bhattacharya, 2005; Hampson et al., 2013). Meanwhile the middle–upper Campanian Castlegate Sandstone is a cliff-forming succession situated above the Blackhawk Formation (Fig. 2a) and is characterized by amalgamated fluvial channel-belt deposits, which are interpreted to preserve braided rivers (e.g., Miall, 1993, 1994). In the middle of the Castlegate Sandstone these sands are less amalgamated, with interbedded mudstones, and are interpreted to preserve more sinuous/meandering channels (e.g., Miall, 1993, 1994). We collected data for the Blackhawk Formation and Castlegate Sandstone from five canyons along the eastern Wasatch Plateau front (Fig. 1a; cf. Lyster et al. (2021)). Dune-scale cross-strata in the Blackhawk Formation are generally associated with bar deposits, as well as lower bar, channel floor or thalweg deposits, whereas dune-scale cross-strata in the Castlegate Sandstone are predominantly associated with bar deposits (Miall, 1993, 1994; Adams and Bhattacharya, 2005; Hampson et al., 2013; Flood and Hampson, 2014).

2.2. Ferron Sandstone, Mancos Shale

The Turonian Ferron Sandstone comprises three deltaic clastic wedges (Cotter, 1971; Chidsey et al., 2004) (Fig. 1b). These deltas were fed by rivers draining the Sevier orogenic front to the WIS

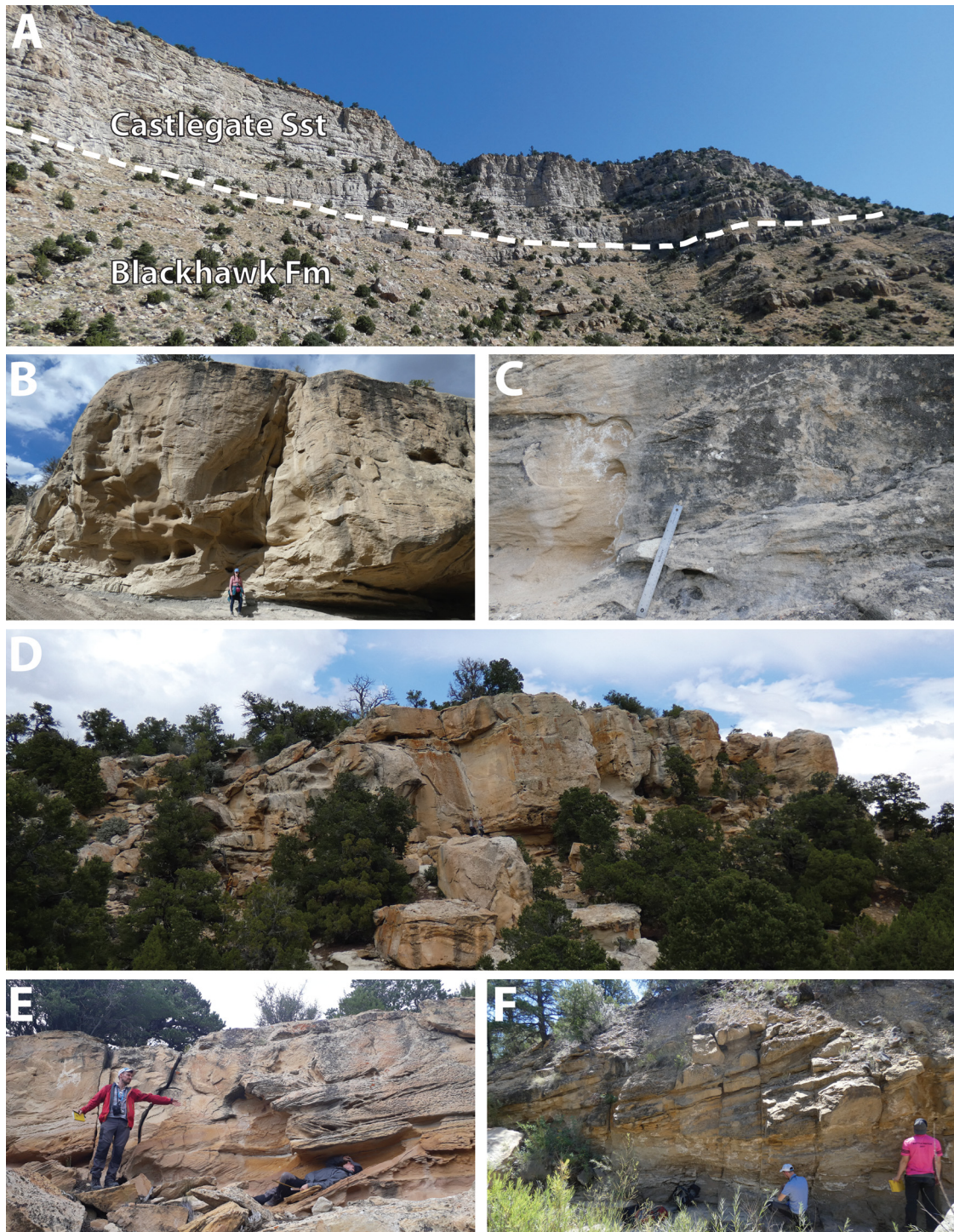


Fig. 2. An overview of Upper Cretaceous fluvial strata from which we collected field data in central Utah, USA. A) Example of typical exposure of the Blackhawk Formation and Castlegate Sandstone (at Salina Canyon; SC; Fig. 1) which crops out in canyons along the eastern Wasatch front. Dashed white line indicates the lithostratigraphic boundary between the Blackhawk Formation and Castlegate Sandstone. Thickness of the Castlegate Sandstone is ca 85 m. B) Example of a major channelized fluvial sandstone body of the Blackhawk Formation at Link Canyon (LC; Fig. 1). C) Crude cross-stratification of amalgamated fluvial deposits of the Castlegate Sandstone at Price Canyon (PC; Fig. 1). D) Example of a major channelized sandstone body of the Ferron Sandstone at Last Chance Creek (LCC; Fig. 1). Persons for scale in centre of image. Thickness of channelized sandstone body in centre of image is ca 12 m. E) Cross-stratified fluvial strata of the Ferron Sandstone at LCC (with some soft-sediment deformation apparent). F) Laterally accreted point bar deposits of the Ferron Sandstone at LCC.

and may have also featured an additional/intermittent longitudinal component of drainage from the south-southwest, as observed for the Blackhawk Formation–Castlegate Sandstone succession (e.g., Szwarc et al., 2015; Pettit et al., 2019). We focus on the Last Chance deltaic complex, using data from three canyons in southwestern Castle Valley (Fig. 1). These canyons preserve the most

palaeo-landward terrestrial fluvial facies of the Last Chance delta and are characterized by major channelized sandstone bodies and abundant floodplain sediments and palaeosols (Cotter, 1971; Chidsey et al., 2004) (Fig. 2d–f). These strata preserve the major meandering trunk channels that fed the Last Chance delta, which is evidenced by abundant laterally accreted point bar deposits (Cot-

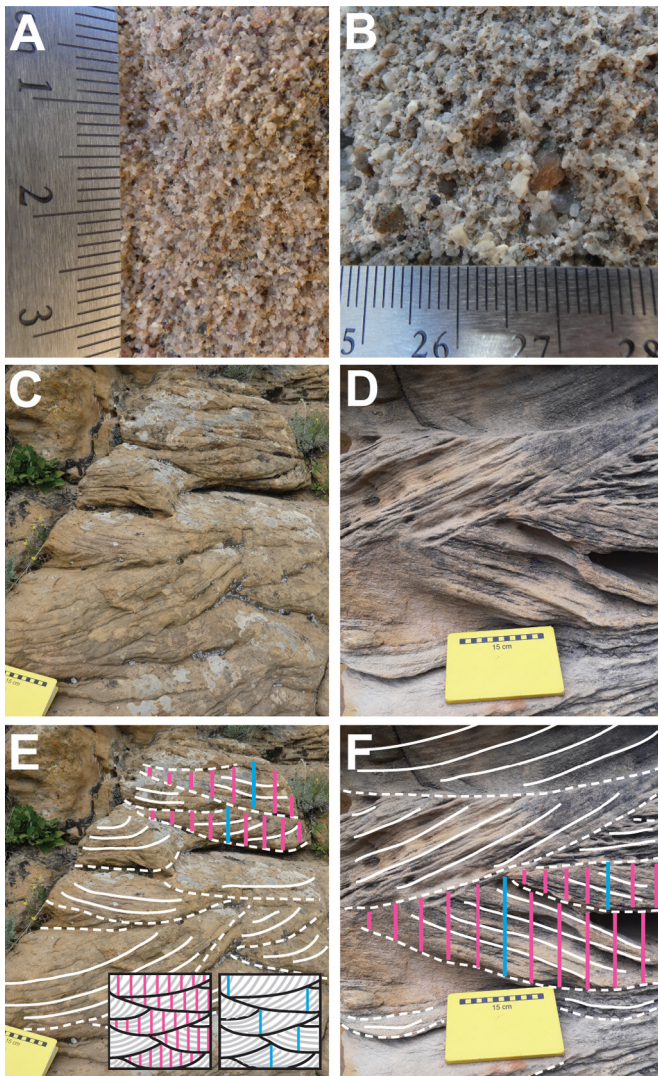


Fig. 3. Field methods. A,B) For each measured cross-set, grain-size was assigned using the Wentworth (1922) classification. C,D) Examples of cross-sets from which distributions of cross-set thicknesses were measured. E,F) Interpreted versions of the images in C,D. Dashed white lines indicate bounding surfaces between cross-sets and solid white lines indicate individual foresets within cross-sets. To exemplify how cross-sets were measured, pink vertical lines indicate the regular spacing within individual cross-sets at which thicknesses were measured, and blue vertical lines indicate where maximum cross-set thicknesses would have been measured for a sample of cross-sets within co-sets at each locality. Insets in E are schematic representations of these two methods of data collection from cross-sets using pink and blue lines, respectively. Figure adapted from Lyster et al. (2021).

ter, 1971; Chidsey et al., 2004) (Fig. 2f). Dune-scale cross-strata in the Ferron Sandstone are generally associated with point bar deposits, as well as lower bar, channel floor or thalweg deposits (Cotter, 1971; Chidsey et al., 2004).

3. Methods

At field localities, we measured the geometries of dune-scale cross-sets. Trough and planar cross-sets occurred predominantly in sand-grade sediments and occasionally in coarser granule-grade sediments (Fig. 3). To measure the distribution of thicknesses within individual cross-sets we delineated cross-set boundaries (i.e., the lower, asymptotic bounding surface and the upper, erosional bounding surface) and measured cross-set thickness with a vertical precision of ± 5 mm at regular intervals along the entire width of the cross-set dip-section ($n=5-15$ measurements) (Fig. 3e,f), in line with methods outlined in Paola and Borgman

(1991), Ganti et al. (2019) and Lyster et al. (2021). We then estimated the median grain-size (D_{50}) using size terms of the Wentworth (1922) classification (Fig. 3a,b). When converted to numerical values, we assigned the middle value for each size term or, where grain-size straddled two size terms, we used the boundary value, e.g., D_{50} of medium-grade sand = 0.375 mm and medium-coarse-grade sand = 0.5 mm (Wentworth, 1922). We repeated this for multiple cross-sets within co-sets. Having measured thickness distributions within individual cross-sets, we then measured a sample of maximum cross-set thicknesses (i.e., the maximum distance between lower and upper bounding surfaces) of cross-sets at each locality ($n \sim 25-75$). These cross-sets were all related, spanning multiple co-sets that were confined, where possible, to a single channelized sandstone body.

For each individual cross-set, we calculated the mean cross-set thickness, h_{xs} , the maximum thickness, and the CV of the internal thickness distribution ($CV(h_{xs})$) – a key parameter to test whether the bedforms are preserved in steady-state or disequilibrium conditions. For each sample of maximum cross-set thicknesses, we similarly calculated the mean maximum cross-set thickness, h_p , and the CV of the entire sample ($CV(h_p)$), and we additionally analysed the shape of each distribution.

We then propagated mean thicknesses of individually measured cross-sets (and their respective grain-sizes) through a well-established quantitative framework (cf. Ganti et al. (2019), Lyster et al. (2021); Supplementary Methods) and used these values to reconstruct bedform turnover timescales – we can use turnover timescales to contextualise the implications of the flood and hierarchy hypotheses. For instance, under the flood hypothesis we expect waning flow durations to be shorter than turnover timescales, whereas under the hierarchy hypothesis we expect bars to be migrating at rates that approach the rates of bedform turnover, i.e., the rates of bedform migration. We reconstructed turnover timescales, T_t , i.e., the time taken to displace the volume of sediment of the bedform (per unit width), following Martin and Jerolmack (2013), Myrow et al. (2018), and Leary and Ganti (2020) as:

$$T_t = \frac{\lambda h_d \beta}{q_b}, \quad (1)$$

where λ is bedform wavelength, which we estimated using the depth scaling relation of van Rijn (1984), h_d is bedform (i.e., dune) height, which we calculated using the relation of Leclair and Bridge (2001), $\beta \sim 0.55$ is the bedform shape factor and q_b is the unit bedload flux. We calculated q_b using the method of Mahon and McElroy (2018), in which q_b is calculated as a function of bed porosity, bedform height, and bedform migration velocity (Supplementary Methods). These methods are consistent with those suggested by Leary and Ganti (2020), but we acknowledge that other approaches could be implemented. As the exact error margins of palaeohydraulic inversion methods are unknown, we used a Monte Carlo uncertainty propagation method to estimate uncertainty, which yielded 10^6 values of T_t per cross-set (Supplementary Methods). From these estimates we extracted median T_t , the 25–75 percentile range of T_t , and the 10–90 percentile range of T_t . For each cross-set, we suggest that the 10–90 percentile range of T_t offers a plausible minimum and maximum value for mean T_t , and that the 25–75 percentile range of T_t offers the bounds in which the true value of mean T_t is most likely to occur.

Reconstruction of T_t included reconstruction of h_d from h_{xs} , which requires a priori knowledge of the bedform preservation ratio (h_{xs}/h_d), which itself is a function of whether bedforms were preserved in steady-state or disequilibrium conditions. To evaluate a maximum T_t value, we used the relation of Leclair and Bridge (2001), in which $h_{xs}/h_d \sim 0.3$, and which assumes steady-state preservation under low bedform climb angle. We then assessed the

sensitivity of T_t to h_{xs}/h_d by repeating the methodology outlined above for h_{xs}/h_d values from 0 to 1. In the absence of preserved formsets that reflect $h_{xs}/h_d \geq 1.0$ (Reesink et al., 2015), enhanced bedform preservation is characterized by $0.3 < h_{xs}/h_d \leq 0.7$ (Supplementary Information; Jerolmack and Mohrig (2005); Reesink et al. (2015); Ganti et al. (2020); Leary and Ganti (2020)). For the sensitivity analyses, we used the h_{xs} and D_{50} of each measured cross-set and calculated the overall mean h_{xs} and mean D_{50} for the Blackhawk Formation, Castlegate Sandstone and Ferron Sandstone, respectively.

4. Results

4.1. Cross-set geometries

We present results aggregated at the formation scale, with no spatial or temporal reference frame, as ancillary field observations suggest there is little variation between field sites (see Supplementary Information and Lyster et al. (2021)). We measured >400 individual dune-scale cross-sets of the Blackhawk Formation ($n = 81$), Castlegate Sandstone ($n = 146$) and Ferron Sandstone ($n = 190$) (Fig. 4), with ~ 5 – 15 thickness measurements per cross-set, totalling >3800 measurements. For each cross-set we recorded grain-size, which is reported in the Supplementary Information, and we calculated the mean thickness and the maximum thickness. Distributions of mean cross-set thicknesses are similar for the Blackhawk Formation and Castlegate Sandstone (two-sample t-test; $p = 0.067$; test statistic = -1.838 ; degrees of freedom = 225); distributions have median values of ~ 0.13 – 0.14 m and 10–90 percentile ranges of 0.10–0.18 m. Distributions of maximum cross-set thicknesses for the Blackhawk Formation and Castlegate Sandstone generally have medians of 0.17–0.18 m and 10–90 percentile ranges of 0.13–0.27 m (Fig. 4a,b). Whereas for the Ferron Sandstone, cross-sets are larger with broader percentile ranges. The distribution of mean cross-set thicknesses has a median of 0.15 m and a 10–90 percentile range of 0.08–0.25 m, and the distribution of maximum cross-set thicknesses has a median of 0.22 m and a 10–90 percentile range of 0.12–0.45 m (Fig. 4c).

We also measured maximum thicknesses of >3000 dune-scale cross-sets across the Blackhawk Formation (801 measurements across 26 samples), Castlegate Sandstone (1015 measurements across 27 samples) and Ferron Sandstone (1257 measurements across 21 samples), with between 25–75 measurements per sample (Fig. 5). For each formation, distributions of maximum thicknesses of cross-sets have median values of ~ 0.20 m (Fig. 5); these values are consistent with maximum values extracted from individually measured cross-sets (Fig. 4). For the Blackhawk Formation and Castlegate Sandstone, 90% of maximum cross-set thicknesses are between ~ 0.15 – 0.30 m, and the upper 10% of maximum cross-set thicknesses are markedly larger (≤ 0.50 – 0.60 m) (Fig. 5a,c). Meanwhile, for the Ferron Sandstone, 90% of maximum cross-set thicknesses are between ~ 0.15 – 0.35 m and the upper 10% of maximum cross-set thicknesses are also markedly larger (≤ 0.70 m) (Fig. 5e). These distributions of maximum cross-set thicknesses across all cross-set samples are generally mirrored in individual cross-set samples (Fig. 5b,d,f), with median values of ~ 0.20 m, suggesting they are not from a limited subset of locations. Most samples of maximum cross-set thicknesses demonstrate positively-skewed, long-tailed distributions wherein relatively few large cross-sets exist among abundant smaller cross-sets (Fig. 5b,d,f). The kurtosis of distributions varies for each formation, such that distributions in the Castlegate Sandstone and Ferron Sandstone are more long-tailed than in the Blackhawk Formation (Fig. 5b,d,f).

Our data show that CV values of cross-set thicknesses are significantly lower than the expected steady-state values of 0.88

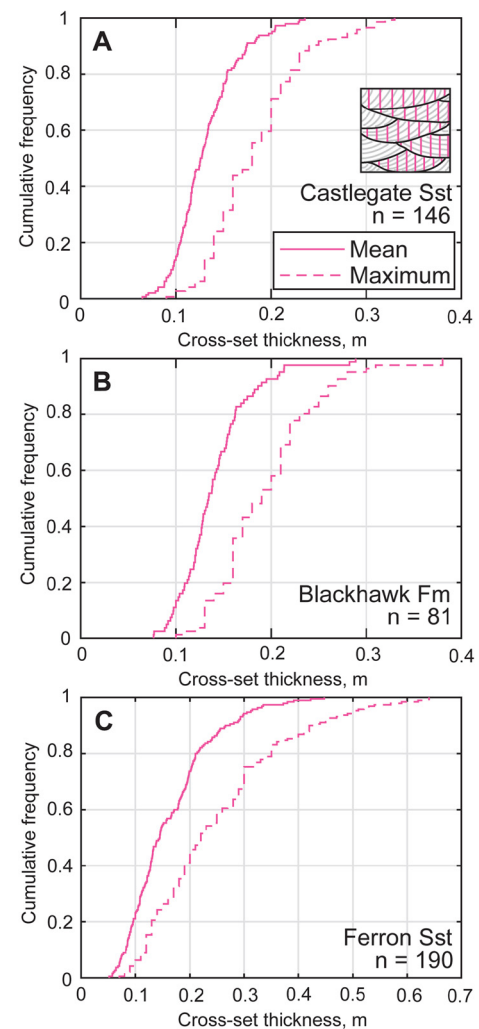


Fig. 4. The cumulative frequency of the mean, median and maximum cross-set thickness for (A) the Castlegate Sandstone, (B) the Blackhawk Formation, and (C) the Ferron Sandstone. The solid pink line indicates the measured mean and the dashed pink line indicates the measured maximum. n indicates the number of cross-sets in which thickness distributions were measured, and therefore the number of cross-sets from which a mean and maximum thickness were subsequently extracted. The inset in A is a schematic representation of how thickness distributions were measured within each cross-set.

(Fig. 6). We found low CV of thicknesses within individual cross-sets ($CV(h_{xs})$), as well as low CV of thicknesses for a sample of measured cross-sets within related co-sets ($CV(h_p)$) (Fig. 6). In the Blackhawk Formation and Castlegate Sandstone, median $CV(h_{xs})$ is 0.3 with a 25–75 percentile range of ~ 0.25 – 0.38 , and maximum $CV(h_{xs})$ extends to 0.45–0.55 (Fig. 6a,b). The Ferron Sandstone $CV(h_{xs})$ values are also low (relative to steady-state) but are higher than in the Blackhawk–Castlegate succession. For the Ferron Sandstone, median $CV(h_{xs})$ is 0.4 with a broader 25–75 percentile range of ~ 0.3 – 0.5 , and maximum $CV(h_{xs})$ extends to 0.6–0.75 (Fig. 6c). We found that none of the measured $CV(h_{xs})$ values were consistent with the proposed empirical range of 0.88 ± 0.30 for steady-state preservation (Bridge, 1997) in the Blackhawk–Castlegate succession; however, 6% of the measurements were within this range for the Ferron Sandstone. For $CV(h_p)$, recovered values are even lower. In the Blackhawk Formation and Castlegate Sandstone median $CV(h_p)$ is 0.2, with 25–75 percentile ranges of ~ 0.15 – 0.25 (Fig. 6a,b), and in the Ferron Sandstone median $CV(h_p)$ is 0.3, with a 25–75 percentile range of ~ 0.25 – 0.35 (Fig. 6c).

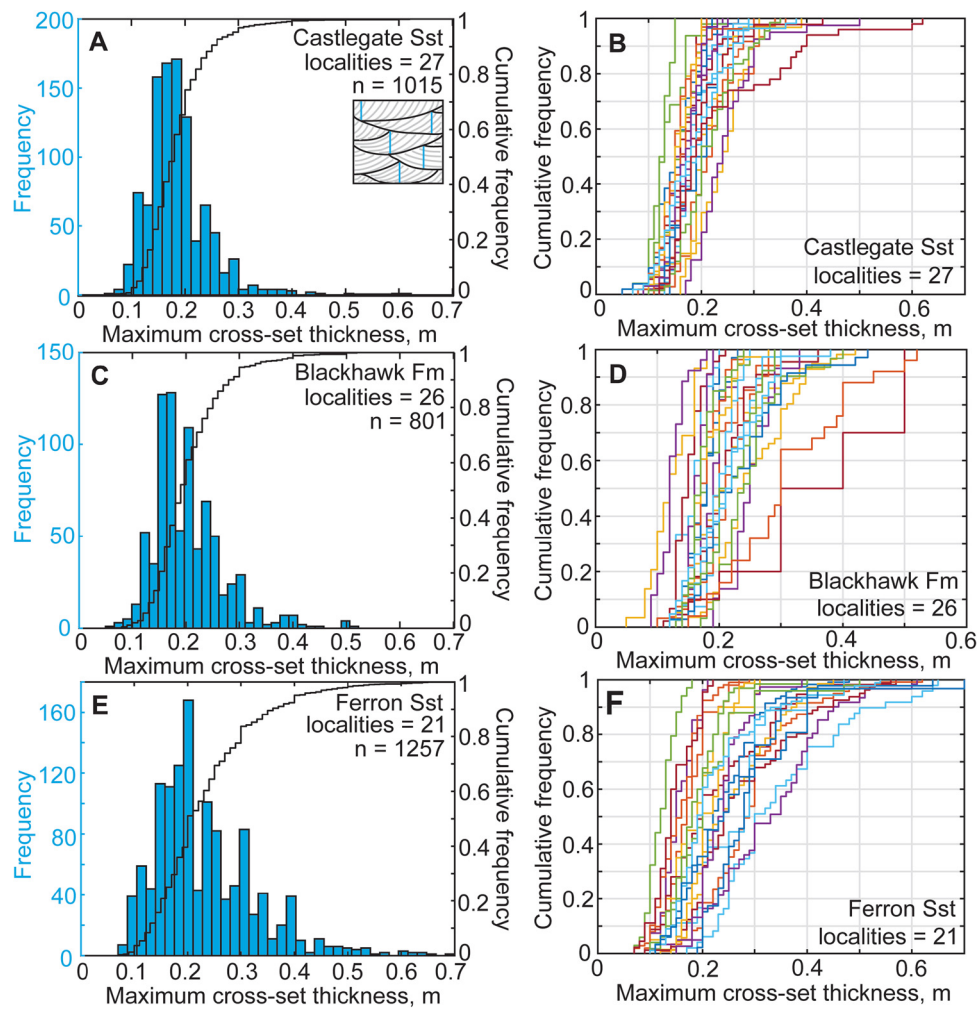


Fig. 5. A) The frequency (left y axis; blue) and cumulative frequency (right y axis; black) of maximum cross-set thicknesses measured across the Castlegate Sandstone. n indicates the total number of cross-sets measured for the entire formation, and the number of localities refers to the field sites across which these measurements were made. Measurements at each locality were for a sample of related cross-sets within cosets, and typically comprised ~ 25 – 75 measurements. B) The cumulative frequency of maximum cross-set thicknesses for each locality within the Castlegate Sandstone. C) The frequency and cumulative frequency of maximum cross-set thicknesses measured across the Blackhawk Formation. D) The cumulative frequency of maximum cross-set thicknesses for each locality within the Blackhawk Formation. E) The frequency and cumulative frequency of maximum cross-set thicknesses measured across the Ferron Sandstone. F) The cumulative frequency of maximum cross-set thicknesses for each locality within the Ferron Sandstone. The inset in A is a schematic representation of how maximum thicknesses were measured across samples of cross-sets.

4.2. Maximum bedform turnover timescales

We first present results for reconstructed T_t values for each formation using a bedform preservation ratio of 0.3, and then explore the sensitivity of T_t to $h_{xs}/h_d > 0.3$ which is expected for the preservation of bedforms under high angles of local bedform climb. The geometries and grain-sizes of measured cross-sets imply that T_t values typically span 1–10 days, with a median value of 2–4 days (Fig. 7). The overall distributions of T_t vary between the geologic formations (Fig. 7). For the Castlegate Sandstone median T_t is 2.5–3 days, with a 10–90 percentile range of 1–7 days (Fig. 7a). For the Blackhawk Formation, values are marginally higher with a median T_t of 3–3.5 days, and a 10–90 percentile range of 1.5–8 days (Fig. 7b). While the Ferron Sandstone has a similar median T_t of 3–3.5 days, it has a much broader 10–90 percentile range spanning < 1 –15 days (Fig. 7c).

We recovered 10^6 values of T_t for each cross-set using a Monte Carlo approach (see Methods and Supplementary Methods) and the results described above present the cumulative distribution function (CDF) of median T_t values for each cross-set (Fig. 7). We also computed the CDFs for the 10th, 25th, 75th and 90th percentiles of T_t values of each cross-set to highlight the plausible range

of values that are consistent with field observations. These CDFs demonstrate that, despite uncertainty in T_t of up to one order of magnitude, the majority of possible T_t values are between 1 and 10 days (Fig. 7). These T_t values suggest that floods with typical recessions > 10 days would have fully equilibrated bedforms, similar to observations in relatively shallow modern rivers (Leary and Ganti, 2020). Further, the estimated maximum T_t of 2–4 days, with an overall span of 1–10 days (Fig. 7) for dune-scale cross-strata in the Blackhawk-Castlegate succession and the Ferron sandstone are consistent with dune migration in modern natural rivers (e.g., Hajek and Straub, 2017; Leary and Ganti, 2020).

4.3. Sensitivity of bedform turnover timescales to bedform preservation ratio

To assess the sensitivity of T_t to h_{xs}/h_d , we systematically varied h_{xs}/h_d for each formation from 0 to 1 (Fig. 8), where the former indicates no preservation and the latter implies complete preservation of formsets. An increase in h_{xs}/h_d corresponds analytically with a decrease in T_t (see Supplementary Methods). For example, increasing h_{xs}/h_d by a factor of 2, from 0.3 to 0.6, reduces T_t by a factor of 5–6 (Fig. 8). Compared to results for $h_{xs}/h_d = \sim 0.3$, the

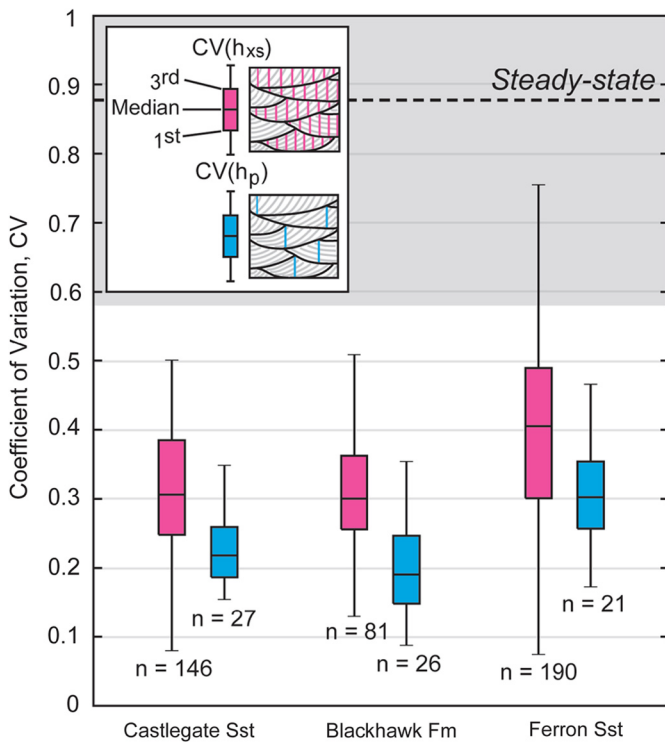


Fig. 6. The coefficient of variation, CV , of cross-set thicknesses measured in the Castlegate Sandstone, Blackhawk Formation, and Ferron Sandstone. Pink boxes indicate CV s of thickness distributions within individually measured cross-sets ($CV(h_{xs})$), with n indicating the number of individually measured cross-sets. The blue boxes indicate CV s of thickness distributions across a sample of (related) cross-sets ($CV(h_p)$), with n indicating the number of field localities at which a sample of cross-set thicknesses was measured. At each locality, the sample of measured cross-sets typically included ~ 25 – 75 cross-sets. Insets within the key demonstrate, schematically, how thicknesses would have been measured for both $CV(h_{xs})$ and $CV(h_p)$ respectively (see Methods). The central mark of each box indicates the median estimate, and the bottom and top edges of each box indicate the 1st and 3rd quartiles (or 25th and 75th percentiles), respectively. The whiskers extend to the most extreme values of CV that are not considered to be outliers. The dashed black line indicates the theoretical steady-state CV of 0.88, following Paola and Borgman (1991), and the grey shaded region indicates the empirical steady-state CV of 0.88 ± 0.30 , following Bridge (1997).

median T_t values for the Castlegate Sandstone and the Blackhawk Formation are smaller by a factor of 5, with median T_t of 0.7 days (~ 17 hours) and 1 day, respectively (Figs. 8a, b). For the Ferron Sandstone, $h_{xs}/h_d = 0.6$ reduces the median T_t by a factor of 6 to ~ 1 day, when compared to $h_{xs}/h_d \sim 0.3$ (Fig. 8c). In all cases, extreme dune preservation with $h_{xs}/h_d = 1$ yielded $T_t < 0.1$ days, and extremely low values of $h_{xs}/h_d \ll 0.3$ yielded unrealistic T_t values as high as 10^5 days (Fig. 8). Experimental bedform preservation under steady and unsteady flows indicates that the h_{xs}/h_d may likely span 0.3 and 0.7 (grey bars, Fig. 8; Supplementary Information) in the absence of evidence for formset preservation (Leary and Ganti, 2020).

5. Discussion

From >400 individually measured dune-scale cross-sets ($n = 5$ – 15 measurements per cross-set) across the three geologic formations, our results indicated that estimated $CV(h_{xs})$ was always lower than 0.88 and ranged from ~ 0.25 – 0.5 (Fig. 6). Across these formations, only 3% of the estimated $CV(h_{xs})$ were consistent with the empirical range of 0.88 ± 0.30 expected for bedform preservation under steady-state conditions (Bridge, 1997). Low $CV(h_{xs})$ is inconsistent with steady-state preservation of bedforms and does not support generation of cross-sets by random variability in scour depths through time (Paola and Borgman, 1991; Leclair and Bridge,

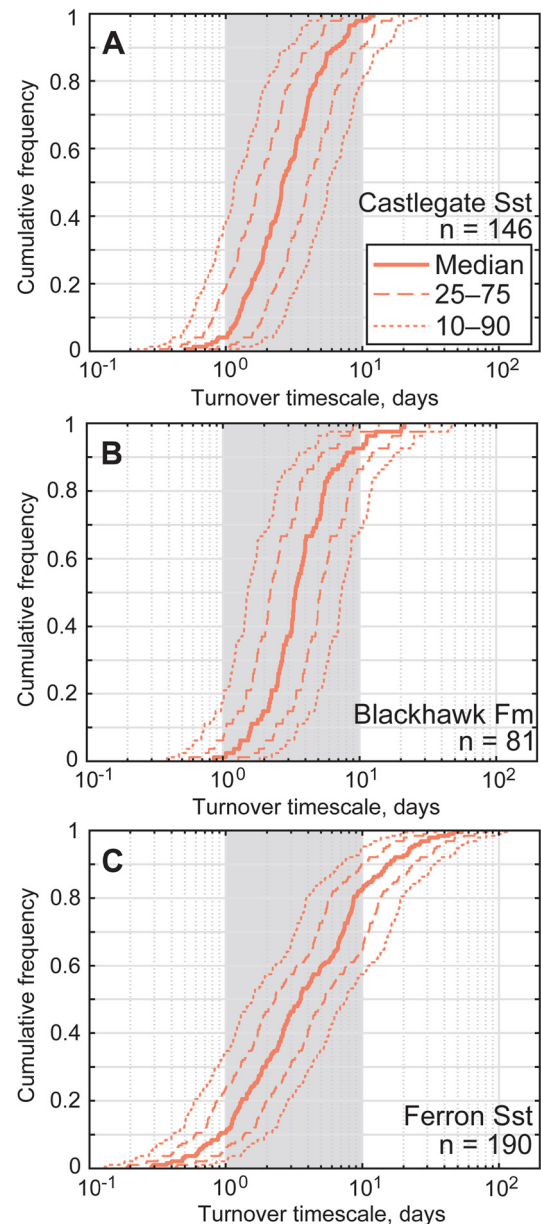


Fig. 7. The cumulative frequency of estimated turnover timescales, T_t , calculated for (A) the Castlegate Sandstone, (B) the Blackhawk Formation, and (C) the Ferron Sandstone (see Supplementary Methods). T_t was calculated for each cross-set from which a cross-set thickness distribution was measured, using the mean thickness and the measured grain-size (Fig. 3; see Methods). n indicates the number of T_t values that were calculated (equal to the number of measured cross-set thickness distributions). The solid orange line indicates the median T_t reconstructed for each cross-set, the dashed orange lines indicate the 25th–75th percentile range of T_t values reconstructed for each cross-set, and the dotted orange lines indicate the 10th–90th percentile range of T_t values reconstructed for each cross-set, which we offer as plausible spreads of values for mean T_t (see Supplementary Methods). Grey shaded region indicates T_t values of 1–10 days; for the Castlegate Sandstone and Blackhawk Formation, ~ 90 – 95% of median T_t values fall within this range and, for the Ferron Sandstone, $\sim 70\%$ of median T_t values fall within this range.

2001; Leclair, 2002; Jerolmack and Mohrig, 2005). Instead, our observations provide evidence for enhanced bedform preservation driven by localized increase in sedimentation rates relative to the bedform migration rates (Jerolmack and Mohrig, 2005; Ganti et al., 2020; Leary and Ganti, 2020), and suggest that river dune deposits of the Blackhawk Formation, Castlegate Sandstone, and Ferron Sandstone are dominated by bedform disequilibrium dynamics. Below we discuss the implications of these observations under the

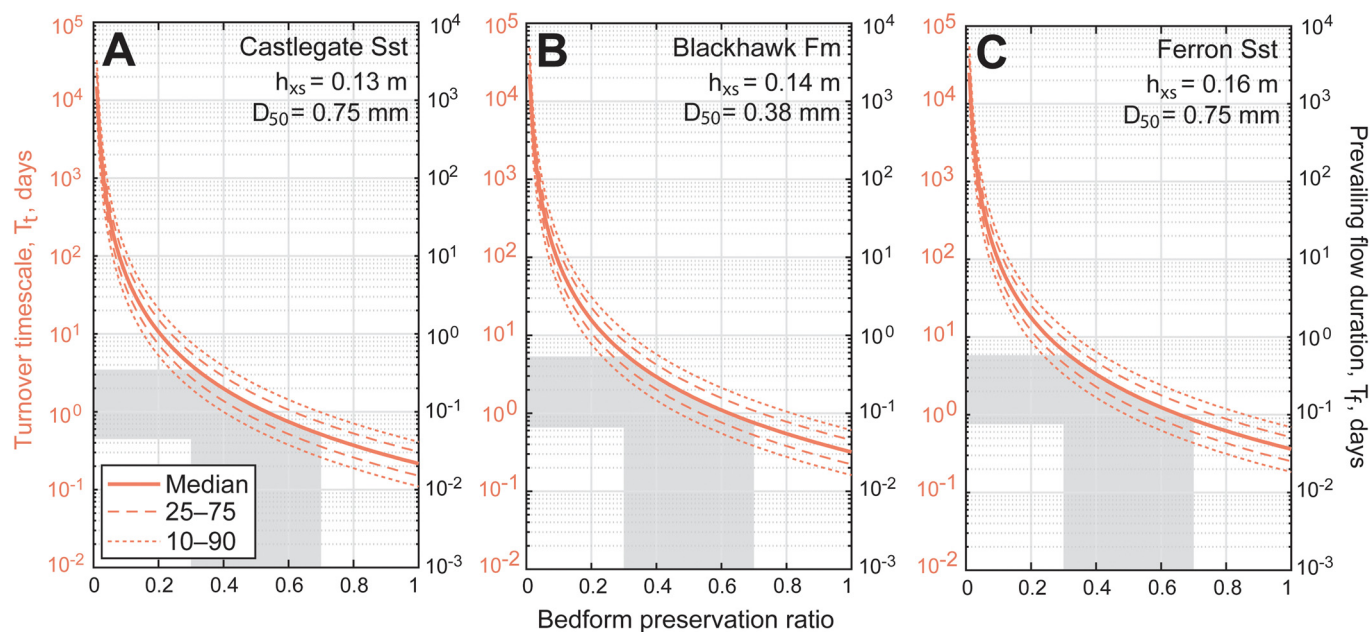


Fig. 8. Turnover timescales, T_t , reconstructed for the Castlegate Sandstone, Blackhawk Formation and Ferron Sandstone using a range of preservation ratios. For these purposes, the mean cross-set thickness (h_{xs}) and median grain-size (D_{50}) for each geologic formation have been used (i.e., the mean and median across all measured cross-set distributions). The solid orange line indicates the median T_t reconstructed for each bedform preservation ratio, the dashed orange lines indicate the 25th–75th percentile range of T_t values reconstructed for each bedform preservation ratio, and the dotted orange lines indicate the 10th–90th percentile range of T_t values reconstructed for each bedform preservation ratio, which we offer as plausible spreads of values for mean T_t (see Supplementary Methods). The grey region highlights the range of median T_t values associated with a plausible range of bedform preservation ratios; steady-state bedform preservation ratios are ~ 0.3 , and Leary and Ganti (2020) documented that higher bedform preservation ratios may extend up to ~ 0.7 during flash floods. On the right y axis, we show reconstructed prevailing flow durations, T_f , for the scenario in which T_f is a factor of 10 smaller than the reconstructed bedform turnover timescale.

flood and hierarchy hypotheses and delineate potential approaches to disentangle their relative roles in ancient fluvial systems.

5.1. Implications of the flood hypothesis for bedform preservation

Using physical experiments, Leary and Ganti (2020) showed that, where bedform disequilibrium dynamics are only controlled by formative flow variability, low $CV(h_{xs})$ indicates a scenario in which the formative flow duration (T_f), i.e., the flood recession, is significantly less than the bedform turnover timescale (T_t). Bedform disequilibrium dynamics associated with formative flow variability typically manifest in rivers with flashy flood hydrographs, in which river discharge is characterized by floods with a short flood recession period relative to T_t (Leary and Ganti, 2020) – the rapid decline in water discharge following peak flood minimizes the time available for bedform reworking and enhances bedform preservation (Leary and Ganti, 2020). Under the flood hypothesis, the documented low $CV(h_{xs})$ is consistent with T_f values that are a factor of 10 smaller than T_t (assuming the ratio of T_f to T_t is ~ 0.1 ; cf. Leary and Ganti (2020)). As the maximum T_t values fall between 1–10 days for our field data, the estimated $CV(h_{xs})$ indicates typical T_f values spanning 0.1–1 day (2.4–24 hours) for $h_{xs}/h_d \approx 0.3$. The range of plausible T_f values consistent with experimentally observed bedform preservation ratios and field-estimated $CV(h_{xs})$ is on the order of 0.1 days for all the geologic formations considered here (Fig. 8).

Under the flood hypothesis, our field data consistently indicate that flood recessions did not exceed a few hours to a day for these Late Cretaceous fluvial systems. Given the typical shape of flashy flood hydrographs, we also anticipate that total flood durations did not exceed a few hours to a few days. Our estimated flood durations are plausible and consistent with recent (decadal-scale) observations of modern rivers in sub-tropical and/or mid-latitude regions (e.g., Serinaldi et al., 2018). Moreover, compilations of global flood data indicate that, for flood durations on the order of

hours to days, the main causes are heavy rain, brief torrential rain, tropical storms, and extra-tropical storms (Serinaldi et al., 2018). These flood durations, and associated causes, are typical of perennial discharge regimes. While the Blackhawk Formation, Castlegate Sandstone and Ferron Sandstone have not been explicitly studied using variable discharge facies models, existing facies analyses of these formations have typically described sedimentary and architectural structures associated with perennial rivers (see review by Plink-Björklund, 2015). These include abundant Froude subcritical structures (i.e., cross-sets from which we collected data; Fig. 3) and well-developed macroforms (i.e., bars and accretion sets) (Cotter, 1971; Miall, 1994; Chidsey et al., 2004; Adams and Bhattacharya, 2005; Hampson et al., 2013; Flood and Hampson, 2014; Chamberlin and Hajek, 2019).

Independent modelling and proxy studies of palaeoclimate for the Late Cretaceous of central Utah suggest the region was subject to a sub-tropical/monsoonal climate with monsoonal precipitation and frequent seasonal flooding in low-lying alluvial plains (e.g., Fricke et al., 2010; Sewall and Fricke, 2013). However, floods caused by monsoonal rains typically have long durations spanning ~ 5 –25 days (Serinaldi et al., 2018). Additionally, an abundance of features associated with monsoonal systems, e.g., in-channel mud layers, abundant soft-sediment deformation, soft-sediment clast conglomerates (see review by Plink-Björklund, 2015), have not been reported in the literature for these formations or observed at our field localities. Given that our reconstructed flood durations and existing facies models indicate perennial discharge regimes, the flood hypothesis indicates that these river dune deposits could record bedform adjustment to flooding associated with storm events as opposed to sustained monsoonal flooding.

5.2. Implications of the hierarchy hypothesis for bedform preservation

Under the alternative hierarchy hypothesis, enhanced bedform preservation is facilitated by self-organization of fluvial systems

into a series of hierarchical elements (Ganti et al., 2020), where the nature of preservation of topography within a given hierarchical level is solely controlled by the next level in the morphodynamic hierarchy. The presence of bars — the higher-order hierarchical elements of dunes — will locally enhance preservation of river dunes because the bars both provide accommodation for bedforms and increase bedform climb angles (Reesink et al., 2015; Ganti et al., 2020). Cardenas et al. (2020) observed low $CV(h_{xs})$ for dune-scale cross-strata on the stoss and lee slopes of point bar and free bar deposits, when compared to dune-scale cross-strata in thalweg deposits of the Cretaceous Cedar Mountain Formation, Utah, which is consistent with the hierarchy hypothesis for bedform preservation. Numerical models indicate that observed low $CV(h_{xs})$ values are associated with rapid sedimentation rates relative to bedform migration rates such that the bedform climb angle is of the order of 10^{-2} to 10^{-1} (Jerolmack and Mohrig, 2005). Given that the local angle of climb for bedforms is influenced by the relative rates of dune migration to bar migration (Ganti et al., 2020), these results suggest low $CV(h_{xs})$ values measured in the field are consistent with timescales of bar migration on the order of days to months.

The nature of stratigraphic architecture, particularly of barform deposits, is well-documented for the Blackhawk Formation, Castlegate Sandstone and Ferron Sandstone (Cotter, 1971; Miall, 1993, 1994; Chidsey et al., 2004; Adams and Bhattacharya, 2005; Hampson et al., 2013; Flood and Hampson, 2014; Chamberlin and Hajek, 2019; Lyster et al., 2021). The Castlegate Sandstone comprises amalgamated fluvial channel-belt deposits which, architecturally, are dominated by barforms (e.g., mid-channel bars) (Miall, 1993, 1994; Chamberlin and Hajek, 2019). Therefore, dune-scale cross-sets that we measured in the Castlegate Sandstone likely preserve dunes that were influenced by bar migration, and it is possible that low $CV(h_{xs})$ values observed in these cross-sets reflect bedform disequilibrium dynamics associated with the hierarchy hypothesis, especially given that unit bar migration rates typical of braided rivers are sometimes comparable to dune migration rates (Strick et al., 2019). Conversely, fluvial strata of the Blackhawk Formation and Ferron Sandstone comprise major channelized sandstone bodies (Cotter, 1971; Chidsey et al., 2004; Adams and Bhattacharya, 2005; Hampson et al., 2013; Flood and Hampson, 2014) which, while abundant in barforms (e.g., laterally accreted point bar deposits; Fig. 2f), also likely preserve a much larger proportion of channel deposits that are devoid of barform architecture, and which may reflect thalweg deposits. Cardenas et al. (2020) hypothesized that thalweg strata represent aggradation in channel beds during the final flood event prior to channel avulsion. We therefore consider that enhanced bedform preservation in thalweg deposits of the Blackhawk Formation and Ferron Sandstone is less likely to reflect bedform preservation in the presence of rapid bar migration and, instead, is more likely to reflect formative flow variability.

5.3. Detangling flood versus hierarchy controls on bedform preservation

While both the flood hypothesis and the hierarchy hypothesis explain the observed dominance of enhanced bedform preservation, disentangling their relative roles in controlling bedform preservation is currently non-trivial. We hypothesize that spatially contextualizing the observed deposits may be critical for evaluating the controls on bedform preservation. For example, it is likely that dunes preserved in channel-thalweg deposits of single-thread rivers are not influenced by the presence of bars and, therefore, may reflect the formative flood variability. This scenario may be similar to physical experiments that do not exhibit the multiple morphodynamic hierarchical levels that typify natural rivers. We hypothesize that, where low $CV(h_{xs})$ values are observed in dune-scale cross-sets associated with thalweg deposits, we can use estimated bedform turnover timescales to constrain formative flow

durations. Similarly, field observations indicate that dunes preserved in the presence of bars are likely to be better preserved than expected under steady-state conditions (Reesink et al., 2015; Cardenas et al., 2020). In this scenario, $CV(h_{xs})$ may yield insight into the relative rates at which bedforms and barforms migrated in ancient fluvial systems.

Together, single-thread river deposits may display a larger range of $CV(h_{xs})$ that reflects both formative flow variability and the relative kinematic rates of evolution of successive hierarchical levels in the morphodynamic hierarchy. In contrast, braided rivers are characterized by relatively rapid migration of unit bars and free bars in the presence of river dunes (e.g., Strick et al., 2019) and detangling the role of morphodynamic hierarchy and flood variability may be more difficult. Our results are consistent with this hypothesis as we observe a larger range of $CV(h_{xs})$ for single-thread river deposits of the Ferron Sandstone compared to the predominantly braided river deposits of the Castlegate Sandstone (Fig. 6). Nonetheless, this work provides a basis for further testing the roles of flow variability and morphodynamic hierarchy on the preservation of bedform dynamics, including other causes of non-uniform flow such as channel abandonment and backwater hydraulics (e.g., Wu et al., 2020).

In terms of cross-set geometries, a promising avenue to decipher the dominant control on bedform disequilibrium dynamics is to compare population statistics of related cross-sets, measured in the field, with those from experimental observations. For instance, Leary and Ganti (2020) showed that, in flashy flood hydrographs, the rapid decline of water discharge associated with short waning-flow durations enhances preservation of relatively larger, peak-flood equilibrated dunes (Leary and Ganti, 2020). In this scenario, we expect maximum cross-set thicknesses to have a positively skewed long-tailed distribution with large cross-sets interspersed with relatively smaller cross-sets (Leary and Ganti, 2020). Whereas bedform preservation in steady-state conditions, or under a broad flood hydrograph, will likely result in maximum cross-set thicknesses that have a short-tailed distribution, with a much higher frequency of smaller cross-sets, as longer waning-flow durations enable reworking of larger dunes such that the preservation potential of peak-flood equilibrated dunes is low (Leclair, 2011; Leary and Ganti, 2020). Across our measured samples, distributions of maximum cross-set thicknesses are consistent with bedform preservation under the flood hypothesis; most samples have long-tailed, positively skewed distributions (Figs. 5b,d,f). Based on these considerations, we judge it plausible that fluvial stratigraphy in the Blackhawk Formation and Ferron Sandstone may record bedform disequilibrium dynamics driven by formative flow variability, associated with the magnitudes and timescales of individual discharge events on the timescale of hours to days. Future experimental and modelling work should investigate whether and how bedform preservation ratios and the statistical nature of preserved cross-sets differs between systems in which bedform disequilibrium dynamics are driven by flashy flood hydrographs versus coevolution of dunes and bars, respectively. We advocate that this is the next step in determining the extent to which discharge variability can be quantitatively reconstructed from stratigraphic observations.

Ultimately, despite sampling a variety of fluvial planform styles across large geographic regions, our results indicate that measured dune-scale cross-sets do not demonstrate the geometries expected for bedform preservation under steady-state conditions, which routinely underpin palaeohydraulic investigations of ancient fluvial systems. This indicates that application of bedform preservation ratios of ~ 0.3 to fluvial strata may result in overestimation of true palaeoflow depths (cf. Leclair and Bridge, 2001) and consequently underestimate palaeoslopes. We argue that systematic measurements of cross-set geometries and, where possible, bedform preservation ratios should be a routine tool to facilitate and

contextualize palaeohydraulic reconstructions, and to test for the presence of bedform disequilibrium dynamics.

6. Conclusions

We made systematic measurements of dune-scale cross-set geometries and grain-sizes in fluvial strata of three Upper Cretaceous geologic formations in central Utah, USA: the Blackhawk Formation, Castlegate Sandstone, and Ferron Sandstone. Across all three formations, we documented consistently low $CV(h_{xs})$ in preserved cross-set thicknesses of 0.25–0.5. These field observations are inconsistent with the steady-state bedform preservation model that assumes cross-sets are generated by random variability in scour depth with time (Paola and Borgman, 1991; Leclair and Bridge, 2001). Instead, our observations add to the growing recognition that bedform preservation is dominated by disequilibrium dynamics (Reesink et al., 2015; Ganti et al., 2020; Leary and Ganti, 2020), resulting in higher bedform preservation ratios and the deposition of cross-sets which preserve a relatively narrow distribution of thicknesses ($CV(h_{xs}) \ll 0.88$).

We considered two independent hypotheses that lead to enhanced bedform preservation in disequilibrium conditions. Under the flood hypothesis, our data indicate that the flood durations that typify these deposits likely ranged from hours to days, which are reflective of heavy rain and tropical storms in these ancient fluvial landscapes. Under the hierarchy hypothesis, the observed low $CV(h_{xs})$ is consistent with bedform deposits preserved with rapidly evolving bars whose timescale of migration likely spans days to months. Detangling the flood versus hierarchy controls on bedform preservation may be possible through the spatial contextualization of preserved deposits of single-thread rivers, with flow variability potentially the dominant control on the nature of bedform preservation in channel-thalweg deposits, such as those observed in the Ferron Sandstone and Blackhawk Formation. However, detangling these relative controls may be difficult in the deposits of braided rivers, such as the Castlegate Sandstone, which are characterized by migration of unit bars and braid bars that can lead to the enhanced bedform preservation.

Where low $CV(h_{xs})$ reflects enhanced bedform preservation associated with formative flow variability, the approaches presented in this paper have significant implications for investigating discharge variability in the geologic past, particularly the magnitudes, transport capacities, and durations of individual flood events generated during short-period climatic perturbations. Meanwhile, where low $CV(h_{xs})$ reflects enhanced bedform preservation associated with the presence of a morphodynamic hierarchy, these results have implications for evaluating the nature of interactions between dunes, bars, channel migration and channel avulsion in palaeo-channel networks. We advocate that quantifying cross-set geometries should become a standard approach in future studies to improve and contextualize palaeohydrological reconstructions from ancient fluvial deposits.

CRediT authorship contribution statement

Sinéad J. Lyster: Conceptualization, Formal analysis, Funding acquisition, Investigation, Methodology, Project administration, Visualization, Writing – original draft. **Alexander C. Whittaker:** Conceptualization, Funding acquisition, Methodology, Supervision, Writing – review & editing. **Elizabeth A. Hajek:** Resources, Supervision, Writing – review & editing. **Vamsi Ganti:** Resources, Supervision, Writing – review & editing.

Data availability

Field data available in the Supplementary Information.

Declaration of competing interest

The authors declare that they have no known competing financial interests or personal relationships that could have appeared to influence the work reported in this paper.

Acknowledgements

This research was primarily funded by a Natural Environment Research Council (NERC) Science and Solutions for a Changing Planet Doctoral Training Partnership (DTP) grant to SJL, with additional funding by The Geological Society of London and The British Sedimentological Research Group to SJL. We thank George Hedley and Bailey Lathrop for support with field data collection, and we thank the Safiya Alpheus for useful discussions. We would also like to thank Luca Colombera and one anonymous reviewer for their constructive reviews, which have greatly improved this manuscript.

Appendix A. Supplementary material

Supplementary material related to this article can be found online at <https://doi.org/10.1016/j.epsl.2021.117355>.

References

- Adams, M.M., Bhattacharya, J.P., 2005. No change in fluvial style across a sequence boundary, Cretaceous Blackhawk and Castlegate formations of central Utah, U.S.A. *J. Sediment. Res.* 75 (6), 1038–1051. <https://doi.org/10.2110/jsr.2005.080>.
- Allen, J.R.L., 1982. *Sedimentary Structures; Their Character and Physical Basis*. Vol. 1, vol. 30. Elsevier, Amsterdam.
- Best, J., 2005. The fluid dynamics of river dunes: a review and some future research directions. *J. Geophys. Res., Earth Surf.* 110 (F4). <https://doi.org/10.1029/2004JF000218>.
- Bradley, R.W., Venditti, J.G., 2017. Reevaluating dune scaling relations. *Earth-Sci. Rev.* 165, 356–376. <https://doi.org/10.1016/j.earscirev.2016.11.004>.
- Bridge, J.S., 1997. Thickness of sets of cross strata and planar strata as a function of formative bed-wave geometry and migration, and aggradation rate. *Geology* 25 (11), 971–974. [https://doi.org/10.1130/0091-7613\(1997\)025<0971:TOSOC>2.3.CO;2](https://doi.org/10.1130/0091-7613(1997)025<0971:TOSOC>2.3.CO;2).
- Cardenas, B.T., Mohrig, D., Goudge, T.A., Hughes, C.M., Levy, J.S., Swanson, T., Mason, J., Zhao, F., 2020. The anatomy of exhumed river-channel belts: Bedform to belt-scale river kinematics of the Ruby Ranch Member, Cretaceous Cedar Mountain Formation, Utah, USA. *Sedimentology* 67 (7), 3655–3682. <https://doi.org/10.1111/sed.12765>.
- Carling, P.A., 1999. Subaqueous gravel dunes. *J. Sediment. Res.* 69 (3), 534–545. <https://doi.org/10.2110/jsr.69.534>.
- Chamberlin, E.P., Hajek, E.A., 2019. Using bar preservation to constrain reworking in channel-dominated fluvial stratigraphy. *Geology* 47 (6), 531–534. <https://doi.org/10.1130/G46046.1>.
- Chidsey, T.C., Adams, R.D., Morris, T.H., 2004. *Regional to Wellbore Analog for Fluvial-Deltaic Reservoir Modeling: The Ferron Sandstone of Utah*, vol. 50.
- Colombera, L., Arévalo, O.J., Mountney, N.P., 2017. Fluvial-system response to climate change: the Paleocene-Eocene Tremp Group, Pyrenees, Spain. *Glob. Planet. Change* 157, 1–17. <https://doi.org/10.1016/j.gloplacha.2017.08.011>.
- Cotter, E., 1971. Paleoflow characteristics of a late Cretaceous river in Utah from analysis of sedimentary structures in the Ferron sandstone. *J. Sediment. Res.* 41, 129–138. <https://doi.org/10.1306/74D72202-2B21-11D7-8648000102C1865D>.
- Edgar, L.A., Gupta, S., Rubin, D.M., Lewis, K.W., Kocurek, G.A., Anderson, R.B., Bell III, J.F., Dromart, G., Edgett, K.S., Grotzinger, J.P., Hardgrove, C., Kah, L.C., Leveille, R., Malin, M.C., Mangold, N., Milliken, R.E., Minitti, M., Palucis, M., Rice, M., Rowland, S.K., Schieber, J., Stack, K.M., Sumner, D.Y., Wiens, R.C., Williams, R.M.E., Williams, A.J., 2018. Shaler: in situ analysis of a fluvial sedimentary deposit on Mars. *Sedimentology* 65 (1), 96–122. <https://doi.org/10.1111/sed.12370>.
- Fielding, C.R., Alexander, J., Allen, J.P., 2018. The role of discharge variability in the formation and preservation of alluvial sediment bodies. *Sediment. Geol.* 365, 1–20. <https://doi.org/10.1016/j.sedgeo.2017.12.022>.
- Flood, Y.S., Hampson, G.J., 2014. Facies and architectural analysis to interpret avulsion style and variability: upper Cretaceous blackhawk formation, Wasatch Plateau, central Utah, U.S.A. *J. Sediment. Res.* 84 (9), 743–762. <https://doi.org/10.2110/jsr.2014.59>.
- Foreman, B.Z., Heller, P.L., Clementz, M.T., 2012. Fluvial response to abrupt global warming at the Palaeocene/Eocene boundary. *Nature* 491, 92–95. <https://doi.org/10.1038/nature11513>.
- Fricke, H.C., Foreman, B.Z., Sewall, J.O., 2010. Integrated climate model-oxygen isotope evidence for a North American monsoon during the Late Cretaceous. *Earth Planet. Sci. Lett.* 289 (1–2), 11–21. <https://doi.org/10.1016/j.epsl.2009.10.018>.

- Ganti, V., Hajek, E.A., Leary, K., Straub, K.M., Paola, C., 2020. Morphodynamic hierarchy and the fabric of the sedimentary record. *Geophys. Res. Lett.* 47 (14), e2020GL087921. <https://doi.org/10.1029/2020GL087921>.
- Ganti, V., Paola, C., Froufroula-Georgiou, E., 2013. Kinematic controls on the geometry of the preserved cross sets. *J. Geophys. Res., Earth Surf.* 118 (3), 1296–1307. <https://doi.org/10.1002/jgrf.20094>.
- Ganti, V., Whittaker, A., Lamb, M.P., Fischer, W.W., 2019. Low-gradient, single-threaded rivers prior to greening of the continents. *Proc. Natl. Acad. Sci. USA* 116 (4), 11652–11657. <https://doi.org/10.1073/pnas.1901642116>.
- Ghinassi, M., Moody, J., Martin, D., 2018. Influence of extreme and annual floods on point-bar sedimentation: inferences from Powder River, Montana, USA. *Geol. Soc. Am. Bull.* 131 (1–2), 71–83. <https://doi.org/10.1130/B31990.1>.
- Hajek, E.A., Straub, K.M., 2017. Autogenic sedimentation in clastic stratigraphy. *Annu. Rev. Earth Planet. Sci.* 45 (1), 681–709. <https://doi.org/10.1146/annurev-earth-063016-015935>.
- Hampson, G.J., Jewell, T.O., Irfan, N., Gani, M.R., Bracken, B., 2013. Modest change in fluvial style with varying accommodation in regressive alluvial-to-coastal-plain wedge: upper Cretaceous blackhawk formation, Wasatch Plateau, central Utah, U.S.A. *J. Sediment. Res.* 83 (2), 145–169. <https://doi.org/10.2110/jsr.2013.8>.
- Herbert, C.M., Alexander, J., Amos, K.J., Fielding, C.R., 2020. Unit bar architecture in a highly-variable fluvial discharge regime: examples from the Burdekin River, Australia. *Sedimentology* 67 (1), 576–605. <https://doi.org/10.1111/sed.12655>.
- Holbrook, J., Wanas, H., 2014. A fulcrum approach to assessing source-to-sink mass balance using channel paleohydrologic parameters derivable from common fluvial data sets with an example from the Cretaceous of Egypt. *J. Sediment. Res.* 84 (5), 349–372. <https://doi.org/10.2110/jsr.2014.29>.
- Jerolmack, D.J., Mohrig, D., 2005. Frozen dynamics of migrating bedforms. *Geology* 33 (1), 57–60. <https://doi.org/10.1130/G20897.1>.
- Kauffman, E.G., Caldwell, W., 1993. The Western Interior Basin in space and time. In: Kauffman, E.G., Caldwell, W. (Eds.), *Evolution of the Western Interior Basin: Geological Association of Canada, Special Paper 39*, pp. 1–30.
- Leary, K.C.P., Ganti, V., 2020. Preserved fluvial cross strata record bedform disequilibrium dynamics. *Geophys. Res. Lett.* 47 (2), e2019GL085910. <https://doi.org/10.1029/2019GL085910>.
- Leclair, S.F., 2002. Preservation of cross-strata due to the migration of subaqueous dunes: an experimental investigation. *Sedimentology* 49 (6), 1157–1180. <https://doi.org/10.1046/j.1365-3091.2002.00482.x>.
- Leclair, S.F., 2011. Interpreting fluvial hydromorphology from the rock record: large-river peak flows leave no clear signature. In: Davidson, S.K., Leleu, S., North, C.P. (Eds.), *From River to Rock Record: The Preservation of Fluvial Sediments and Their Subsequent Interpretation*, vol. 97. SEPM Society for Sedimentary Geology.
- Leclair, S.F., Bridge, J.S., 2001. Quantitative interpretation of sedimentary structures formed by river dunes. *J. Sediment. Res.* 71 (5), 713–716. <https://doi.org/10.1306/2DC40962-0E47-11D7-8643000102C1865D>.
- Lyster, S.J., Whittaker, A.C., Hampson, G.J., Hajek, E.A., Allison, P.A., Lathrop, B.A., 2021. Reconstructing the morphologies and hydrodynamics of ancient rivers from source to sink: Cretaceous Western Interior Basin, Utah, USA. *Sedimentology* 68 (6), 2854–2886. <https://doi.org/10.1111/sed.12877>.
- Mahon, R.C., McElroy, B., 2018. Indirect estimation of bedload flux from modern sand-bed rivers and ancient fluvial strata. *Geology* 46 (7), 579–582. <https://doi.org/10.1130/G40161.1>.
- Martin, R.L., Jerolmack, D.J., 2013. Origin of hysteresis in bed form response to unsteady flows. *Water Resour. Res.* 49 (3), 1314–1333. <https://doi.org/10.1002/wrcr.20093>.
- Miall, A.D., 1993. The architecture of fluvial-deltaic sequences in the upper mesaverde group (upper Cretaceous), book cliffs, Utah. In: Best, J.L., Bristow, C.S. (Eds.), *Braided Rivers*, vol. 75. Geological Society, London, pp. 305–332. *Special Publications*.
- Miall, A.D., 1994. Reconstructing fluvial macroform architecture from two-dimensional outcrops; examples from the Castlegate Sandstone, Book Cliffs, Utah. *J. Sediment. Res.* 64 (2b), 146–158. <https://doi.org/10.1306/D4267F78-2B26-11D7-8648000102C1865D>.
- Myrow, P.M., Jerolmack, D.J., Perron, J.T., 2018. Bedform disequilibrium. *J. Sediment. Res.* 88 (9), 1096–1113. <https://doi.org/10.2110/jsr.2018.55>.
- Paola, C., Borgman, L., 1991. Reconstructing random topography from preserved stratification. *Sedimentology* 38 (4), 553–565. <https://doi.org/10.1111/j.1365-3091.1991.tb01008.x>.
- Pettit, B.S., Blum, M., Pecha, M., McLean, N., Bartschi, N.C., Saylor, J.E., 2019. Detrital-zircon U-Pb paleodrainage reconstruction and geochronology of the Campanian Blackhawk–Castlegate succession, Wasatch Plateau and Book Cliffs, Utah, U.S.A. *J. Sediment. Res.* 89 (4), 273–292. <https://doi.org/10.2110/jsr.2019.18>.
- Plink-Björklund, P., 2015. Morphodynamics of rivers strongly affected by monsoon precipitation: review of depositional style and forcing factors. *Sediment. Geol.* 323, 110–147. <https://doi.org/10.1016/j.sedgeo.2015.04.004>.
- Reesink, A.J.H., Van den Berg, J.H., Parsons, D.R., Amsler, M.L., Best, J.L., Hardy, R.J., Orfeo, O., Szupiany, R.N., 2015. Extremes in dune preservation: controls on the completeness of fluvial deposits. *Earth-Sci. Rev.* 150, 652–665. <https://doi.org/10.1016/j.earscirev.2015.09.008>.
- Romans, B.W., Castellort, S., Covault, J.A., Fildani, A., Walsh, J.P., 2016. Environmental signal propagation in sedimentary systems across timescales. *Earth-Sci. Rev.* 153, 7–29. <https://doi.org/10.1016/j.earscirev.2015.07.012>.
- Serinaldi, F., Loecker, F., Kilsby, C.G., Bast, H., 2018. Flood propagation and duration in large river basins: a data-driven analysis for reinsurance purposes. *Nat. Hazards* 94 (1), 71–92. <https://doi.org/10.1007/s11069-018-3374-0>.
- Sewall, J.O., Fricke, H.C., 2013. Andean-scale highlands in the Late Cretaceous Cordillera of the North American western margin. *Earth Planet. Sci. Lett.* 362, 88–98. <https://doi.org/10.1016/j.epsl.2012.12.002>.
- Straub, K.M., Duller, R.A., Foreman, B.Z., Hajek, E.A., 2020. Buffered, incomplete, and shredded: the challenges of reading an imperfect stratigraphic record. *J. Geophys. Res., Earth Surf.* 125 (3), e2019JF005079. <https://doi.org/10.1029/2019JF005079>.
- Strick, R.J.P., Ashworth, P.J., Sambrook Smith, G.H., Nicholas, A.P., Best, J.L., Lane, S.N., Parsons, D.R., Simpson, C.J., Unsworth, C.A., Dale and, J., 2019. Quantification of bedform dynamics and bedload sediment flux in sandy braided rivers from airborne and satellite imagery. *Earth Surf. Process. Landf.* 44 (4), 953–972. <https://doi.org/10.1002/esp.4558>.
- Szwarc, T.S., Johnson, C.L., Stright, L.E., McFarlane, C.M., 2015. Interactions between axial and transverse drainage systems in the Late Cretaceous Cordilleran foreland basin: evidence from detrital zircons in the Straight Cliffs Formation, southern Utah, USA. *Geol. Soc. Am. Bull.* 127 (3–4), 372–392. <https://doi.org/10.1130/B31039.1>.
- Ten Brinke, W.B.M., Wilbers, A.W.E., Wesseling, C., 1999. Dune growth, decay and migration rates during a large-magnitude flood at a sand and mixed Sand-Gravel bed in the Dutch Rhine river system. In: Smith, N.D., Rogers, J. (Eds.), *Fluvial Sedimentology VI*, pp. 15–32.
- van Rijn, L.C., 1984. Sediment transport III: bedforms and alluvial roughness. *J. Hydraul. Eng.* 110 (12), 1733–1754. [https://doi.org/10.1061/\(ASCE\)0733-9429\(1984\)110:12\(1733\)](https://doi.org/10.1061/(ASCE)0733-9429(1984)110:12(1733)).
- Wang, R., Colombero, L., Mountney, N.P., 2020. Palaeohydrological characteristics and palaeogeographic reconstructions of incised-valley-fill systems: insights from the Namurian successions of the United Kingdom and Ireland. *Sedimentology* 67 (7), 3844–3873. <https://doi.org/10.1111/sed.12773>.
- Wentworth, C.K., 1922. A scale of grade and class terms for clastic sediments. *J. Geol.* 30 (5), 377–392. <https://doi.org/10.1086/622910>.
- Wu, C., Nittrouer, J.A., Swanson, T., Ma, H., Barefoot, E., Best, J., Allison, M., 2020. Dune-scale cross-strata across the fluvial-deltaic backwater regime: preservation potential of an autogenic stratigraphic signature. *Geology* 48 (12), 1144–1148. <https://doi.org/10.1130/G47601.1>.
- Wysocki, N., Hajek, E.A., 2021. Mud in sandy riverbed deposits as a proxy for ancient fine-sediment supply. *Geology* 49 (8), 931–935. <https://doi.org/10.1130/G48251.1>.